"LOW COST" APPROACHES FOR THE PREDICTION OF ROTATING INSTABILITIES IN THE VANELESS DIFFUSER OF A RADIAL FLOW PUMP

Banglun ZHOU[1], Antoine DAZIN[2], Annie-Claude BAYEUL-LAINÉ[2*], Jianping YUAN[1], Yaguang HENG[2]
Patrick DUPONT[3], Najib OUARZAZI[4]

[1]National Research Center of Pumps, Jiangsu University, 301,Road Xuefu, Zhenjiang City, 212013, China.
zblujs@163.com, yh@ujs.edu.cn

[2]Laboratoire de Mécanique de Lille (FRE CNRS 3723), ENSAM, 8 Bd Louis XIV, 59034 Lille Cedex, France
Antoine.dazin@ensam.eu, Annie-Claude.bayeul-laine@ensam.eu, Yaguang.heng@ensam.eu

[3]Ecole Centrale de Lille, LML Laboratory, CNRS UMR 8107
Patrick.dupont@centralelille.fr

[4]Universite´ Lille Nord de France, 59000 Lille, France.
najib.ouarzazi@univ-lille1.fr

KEY WORDS

Vaneless diffuser, Radial flow pump, Rotating instability, 2D numerical simulation, Experiment, Linear Stability Analysis.

ABSTRACT

The instabilities, occurring in pumps operating at partial flow rates, may directly cause several negative effects, such as vibration, noise, mechanical damage. The present study is focused on the investigation of the instabilities developing in the vaneless diffuser of a radial flow pump. The prediction of this kind of complex phenomena by numerical simulation usually involves complex (3D unsteady) and expensive calculations. The main goal of this paper is to propose and evaluate some "low cost" numerical or analytical approaches to predict the arising and the characteristics of rotating stall instabilities. For that purpose, two-dimensional numerical unsteady calculations were used. The boundary condition for the diffuser inlet was based on the flow field at the impeller outlet and static pressure was set at the diffuser outlet. The simulations have been managed for several flow rates conditions. The results of the numerical simulation are discussed and compared to i/ an already existing database (including PIV and pressure measurements), ii/ results of a 2D linear stability analysis.

1. INTRODUCTION

Instabilities could appear in pumps and compressors operating at off design conditions. They directly cause negative effects to them, such as vibrations, noise, mechanical damages. Consequently, they could lead to a reduction of the operating range of the machines.
In the last decades, researchers[1-4] have developed theoretical analysis and experiment methods to investigate the mechanism of rotating stall in centrifugal machines. It seems that the physical mechanism associated with vaneless diffuser rotating stall is depending on its geometry. In narrow vaneless diffusers ($h/R_3<0.1$ where h is the diffuser height and R_3 the inlet radius of diffuser), the occurrence of rotating stall is affected by the three-dimensional wall boundary layers [5-7]. In wide diffusers ($h/R_3>0.1$), the wall boundary has no effect on the occurrence of rotating stall, and the instability develops in the core flow between the two

* Corresponding author

boundary layers. In this case, the development of the instability is clearly linked to the value of the absolute flow angle at diffuser inlet [8-9]. It has been shown that a critical value of this angle exists, under which, the instability develops. More recent experiments, including PIV and pressure measurements, were performed, in order to obtain the characteristics of this unstable phenomenon, for many operating conditions [10-13] and compared to 3D unsteady numerical calculations of the whole machine [12]. This last work has shown the ability of this kind of calculations to predict the occurrence and the characteristics of the rotating stalls (the number of cells, the structure of the rotating cells, the pattern and the amplitude of the phenomenon). The main drawback is that they are long and expensive calculations.

In recent years, simplified numerical approaches, based on a 2D numerical simulation of the radial diffuser, were used to predict the behavior of rotating stall in the vaneless diffuser (S. Ljevar [14-15] and Dazin et al [10]). The calculations were based on the Reynolds Averaged Navier-Stokes (RANS) equations, assuming the hypothesis that the flow is two-dimensional in the core flow. The fluid is assumed viscous and incompressible. They showed the ability of such simplified approach to be able to predict the occurrence of the rotating instability. Besides, Tsujimoto et al [8], and more recently Heng et al [16] have used linear stability analysis, assuming that the flow in the vaneless diffuser is 2D, incompressible and non viscous to predict the occurrence of unstable modes in vaneless diffusers.

The aim of the present paper is to evaluate the ability of a 2D simplified approach to predict the occurrence and the characteristics of the rotating stall in a vaneless diffuser. To do so, 2D numerical calculations, similar to the one proposed by S. Ljevar [14-15] and Dazin et al [10], were managed to calculate the rotating instabilities inside a vaneless diffuser of a radial flow pump. A two-dimensional viscous incompressible flow model is used, so the influence of the wall boundary layers are consequently neglected. The boundary condition of the diffuser inlet was based on the flow field at the impeller outlet. A static pressure was set to the diffuser outlet. Monitoring points were located in the diffuser at different radius to acquire the pressure signals. The classical Fourier analysis was applied to identify the spectral characteristics of the developing rotating instabilities. The calculation results are compared to a 2D linear stability analysis results coming from [16] and from experimental results [11-12].

2. EXPERIMENTAL CONFIGURATION

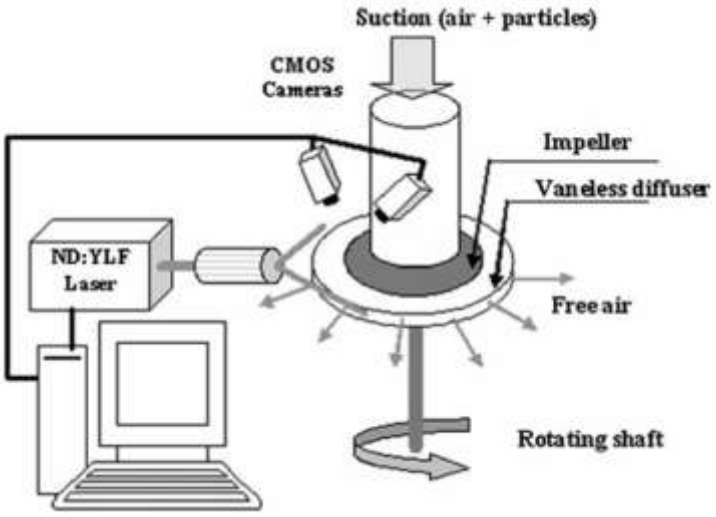

Figure 1 The experimental configuration used in previous works by Dazin et al [11-12]

The experimental measurements, support of the present work, have been carried out in air, in a radial flow pump with a radial impeller and a vaneless diffuser. The test rig used is shown in Figure 1. In order to ensure the axisymmetry of the pressure field at the diffuser outlet, no volute has been installed downstream of the diffuser. The vaneless diffuser walls are in transparent plexiglass, in order to have an optical access for the use of the particle image velocimetry (PIV) technique. Four Brüel & Kjaer condenser microphones (Type 4135) were used to acquire the unsteady pressure data. Their locations were set at two different radii

(R=270mm and 370mm) and two different angle positions (an angle difference of 75°) on the diffuser wall. The experimental measurements is described in detail in [10-11].

The characteristics of the impeller and of the diffuser are given in Table 1. The diffuser's radius ratio is R_4/R_3=1.5 . The vaneless diffuser is considered as a wide vaneless diffuser when h/R_3>0.1.

Impeller characteristics			Units
Outlet radius	R_2	256.6	mm
Tip inlet radius	R_1	141.1	mm
Number of blades	Z	7	
Exit blade height	b_2	38.5	mm
Outlet blade angle	β_2	22.5	deg
Nominal speed of rotation speed	N	1200	rpm
Design flow rate	Q_d	0.236	m^3/s
Reynolds number	Re	7.86×10^5	
Diffuser characteristics			
Inlet Radius	R_3	257.1	mm
Oultet Radius	R_4	390	mm
Constant height	h	40	mm

Table 1: Pump characteristics

3. LINEAR STABILITY ANALYSIS

A 2D linear stability analysis diffuser was applied to study the stability of the flow in the diffuser. The analysis is based on the assumptions of a 2D, non-viscous flow with axisymmetric boundary conditions at the inlet and constant pressure at the outlet. The detail of the methodology used to predict the flow stability is available in the Tsujimoto's paper [8]. According to the linear stability analysis, for a given diffuser's radius ratio R_4/R_3 and a given number of unstable modes *n* (where n reprensents the number of unstable cells), the rotating stall occurs when the absolute flow angle at the diffuser's inlet is below a limit which is called the critical flow angle α_{cr}.Figure 2 represents the evolution of the critical angle, for each mode, as a function of the radius ratio. In the experimental results, the radius ratio is R_4/R_3=1.5. For example, if we consider the flow rate Q/Q_d=0.26, the inlet flow angle is estimated to be α=3 °, by the calculation of the velocity triangle at diffuser's inlet. The analysis of Figure 2 shows that, for this inlet flow angle, all modes (*n*=1-4) are predicted to be unstable.

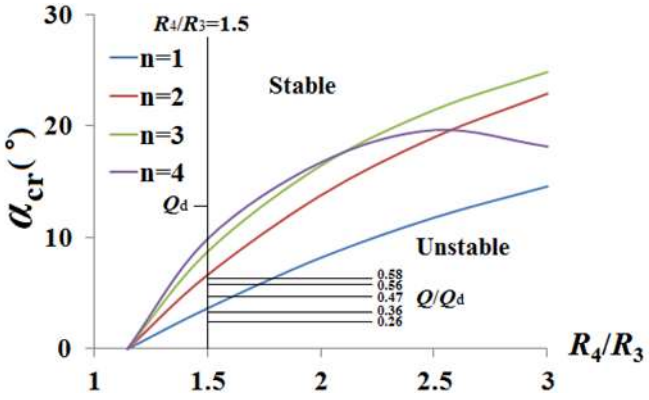

Figure 2. Critical flow angle versus diffuser ratio.

Moreover, the linear stability analysis, when the flow is unstable, is able to predict the propagation speed of the rotating cells. The results of this analysis will be compared to experimental results and to some numerical calculations that will be presented in the following paragraph.

4. NUMERICAL CALCULATIONS

4.1 Turbulence model

The calculations are based on the unsteady Reynolds Averaged Navier-Stokes (URANS) equations with the SST k-ω turbulence model. In this case, the ratio between the diameter of diffuser's outlet and those of the diffuser's inlet is equal to 1.5, the same as in the experiments. The flow field calculated in the present work is 2D and limited to the vaneless diffuser.

The boundary condition at the inlet is an axisymmetric velocity. The tangential and the radial velocity's components at diffuser's inlet are given according to the the flow field at impeller's outlet. It is assumed that the outlet of the vaneless diffuser is connected to free air with a constant static pressure. The turbulence's intensities at the diffuser inlet and outlet are based on the Reynolds number at the inlet and the outlet respectively. For the discretization of the time-dependent terms, the second-order implicit time integration is used and the convergence criteria are 10^{-5}. The time step is 0.00012 s (Corresponding to 360 time steps per impeller revolution). The flow field in the diffuser is considered viscous and incompressible.

The velocities's triangle at the outlet of impeller (Figure 3) is determined to obtain the tangential velocity of the diffuser inlet considering the slip factor. The radial velocity of diffuser's inlet is calculated from the flow rate by equation (2). The slip factor is defined in equation(1). The tangential velocity is evaluated by equation (3).

$$\sigma = 1 - \frac{\pi}{Z} sin\beta_2 \tag{1}$$

$$v_r = \frac{Q}{\pi D_2 b_2 (1 - \frac{Z S_u}{\pi D_2})} \tag{2}$$

$$v_\theta = u_2 - \frac{v_r}{tan\beta_2} - (1-\sigma)u_2 \tag{3}$$

Where σ denotes the slip factor, Z the number of impeller's blades, Q the flow rate, S_u the thickness of impeller's blades at the outlet, D_2 the impeller's outlet diameter.

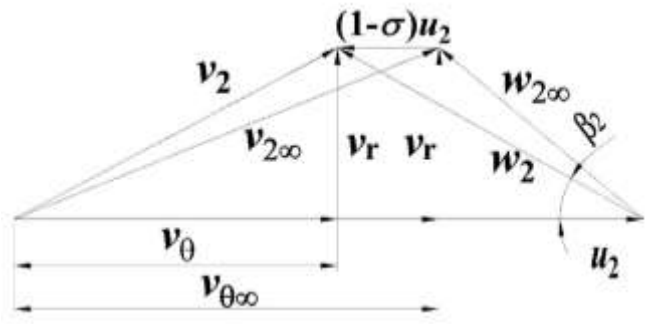

Figure 3 Velocities' triangle at impeller's outlet

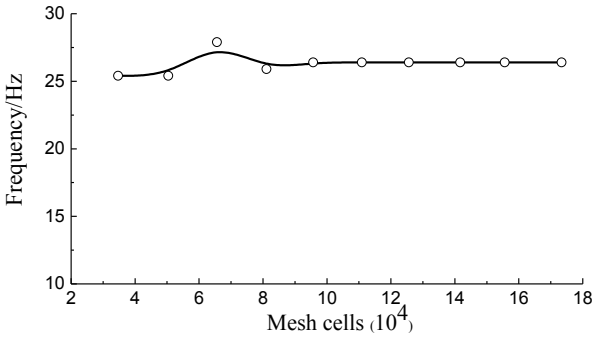

Figure 4 The dominant frequency of static pressure fluctuations for different mesh sizes at Q/Q_d=0.46

4.2 Mesh independence checking

The mesh used is a curvilinear orthogonal grid as shown in Figure 5. A mesh independence analysis has been conducted at flow rate Q/Q_d=0.46. Two monitoring points, located at two radii (R=270mm and R=320mm) and at the same azimuthal position in the diffuser allow to acquire the static pressure evolution. A Fourier analysis is applied to identify the spectral characteristics of the fluctuating pressure. The dominant frequency of the spectrum as a function of the number of mesh-cells is shown in Figure 4. It can be seen that the value of the dominant frequency is constant when the grid size is larger than 95 000. The amplitude of the dominant peak in the spectrum is plotted as a function of the mesh size for the two sensor locations in Figure 6a and 6b. For a number of mesh cells higher than 125 000, the pressure's amplitude remains nearly constant. Finally, the best optimized mesh cells number is 125 000. This mesh will be used for the other simulations presented in this paper.

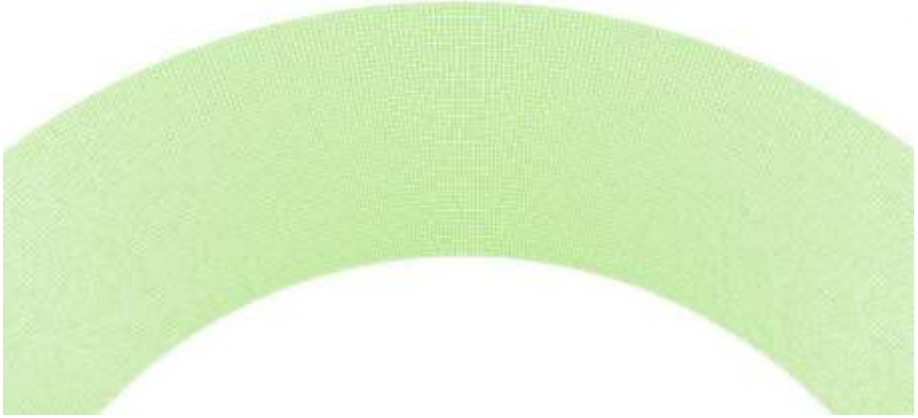

Figure 5 The diffuser's grid

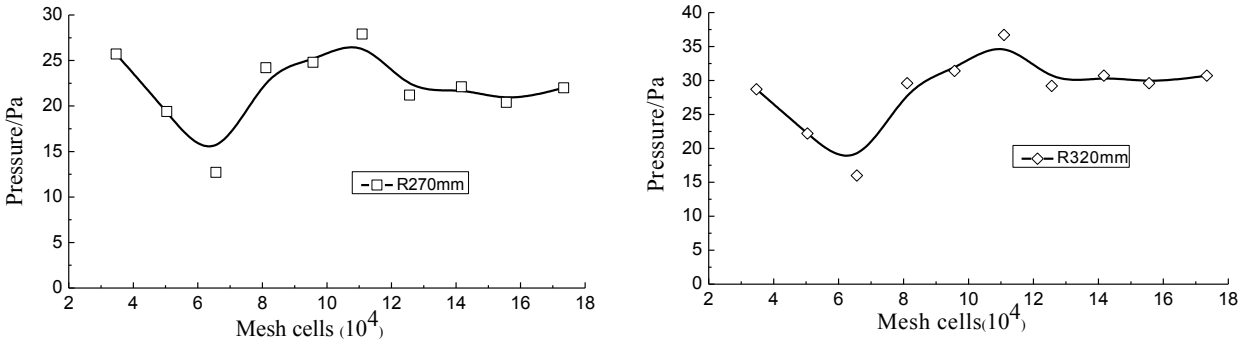

(a) R=270mm (b) R=320mm

Figure 6 The amplitude of the peak spectrum for the dominant frequency at Q/Q_d=0.46

5. RESULTS AND DISCUSSION

5.1 Simulation results

Some of the numerical results obtained are presented in Figures 7 and 8. These figures present the instantaneous flow structures after the development of the instability, in terms of vorticity fields (Figure 7) and velocity fields (Figure 8 and 9). These results confirm, the ability of this kind of calculation to predict the arising of a rotating instability in a radial vaneless diffuser. This instability is characterised by a number of cells which is varying with the flow rate (n=3 for Q/Q_d=0.26 and n = 4 for Q/Q_d =0.31 and Q/Q_d =0.61, in Figures 7, 8 and 9). The unstable cell is characterised by a vortical core which is rotating around the diffuser at a velocity which is a fraction of the impeller velocity. This result is in a good agreement with results obtained Dzine et al, Ljvar et al [10, 14-15]. Considering the radial velocity of the flow, it can be seen that the vortical core is composed of one region of inward velocity next to a region of outward velocity (Figure 8). Between these two regions, a zone of high tangential velocity can be identified near to the diffuser inlet.

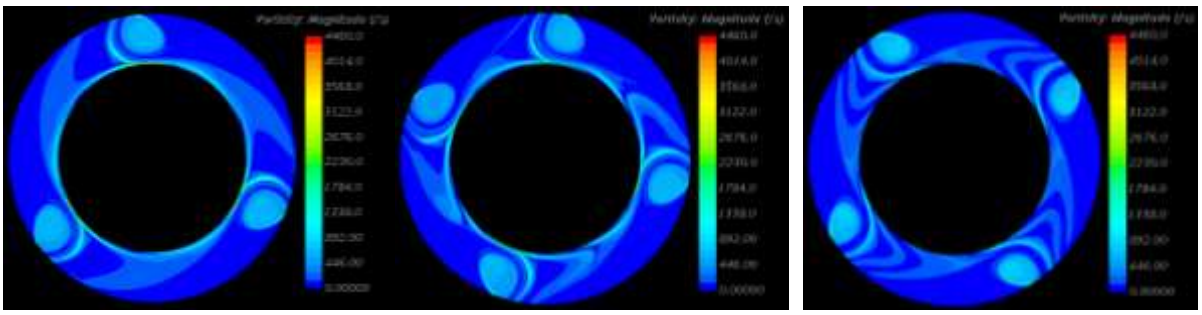

(a) Q/Q_d=0.26 (b) Q/Q_d=0.31 (c) Q/Q_d=0.61

Figure 7 Vorticity magniture fields under different flow rates conditions

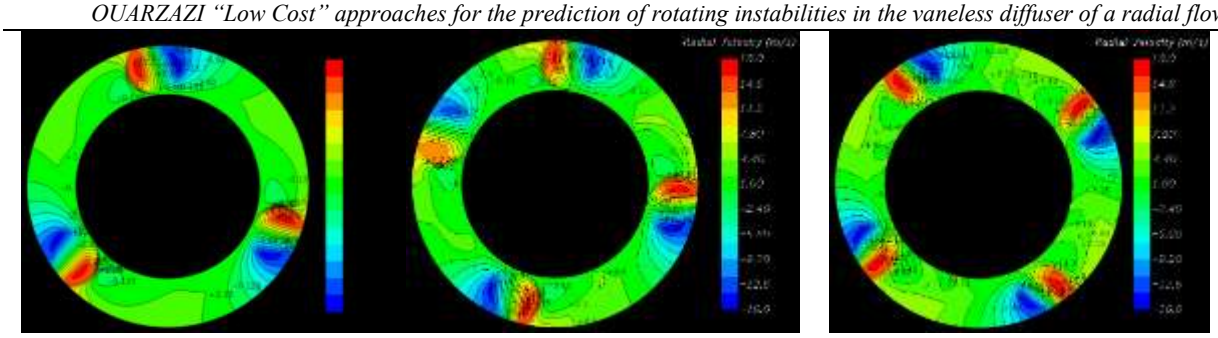

(a) Q/Q_d=0.26 (b) Q/Q_d=0.31 (c) Q/Q_d=0.61

Figure 8 The radial velocity for different flow rates conditions

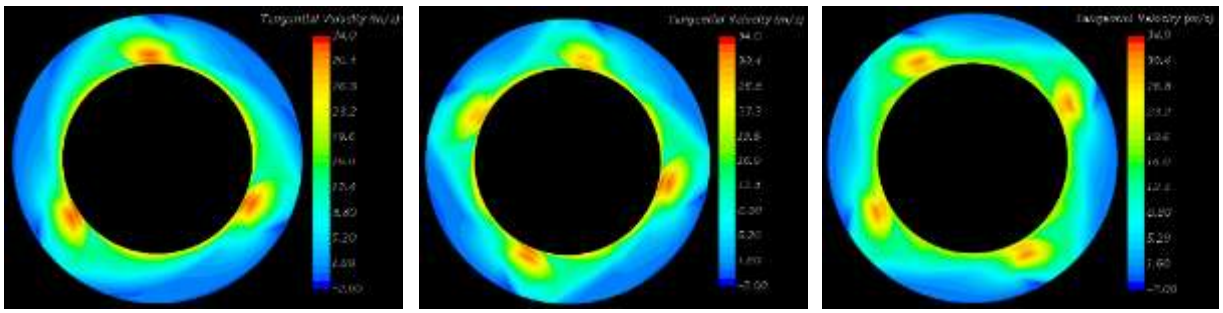

(a) Q/Q_d=0.26 (b) Q/Q_d=0.31 (c) Q/Q_d=0.61

Figure 9 The tangential velocity for different flow rates conditions

In order to deeply understand the mechanism of the rotating stall, the classical Fourier analysis was applied to identify the spectral characteristics of the developing rotating instabilities. The static pressure coefficient Ψ is defined as:

$$\Psi = \frac{p}{\frac{1}{2}\rho u_2^2}$$

Where p is the static pressure, ρ is the flow density, u_2 is the impeller tip tangential velocity. Figure 10 shows the spectra of the rotating stall for the flow rate Q/Q_d=0.26. The monitoring point of static pressure was located on radius R=270mm. The highest peack value of the spectral in simulation (shown in Figure 10 (b)) is in good agreement with the experimental one (shown in Figure 10 (a)). In the calculation, the dominant frequency is 20.4 Hz (the impeller rotation frequency is 20 Hz) for Q/Q_d=0.26 condition, when the three stall cells are observed. So, the fundamental frequency of the rotating stall is 6.8 Hz. This result is quite close to the experimental one (the fundamental frequency of the rotating stall is 5.6 Hz) given by Dazin [10].

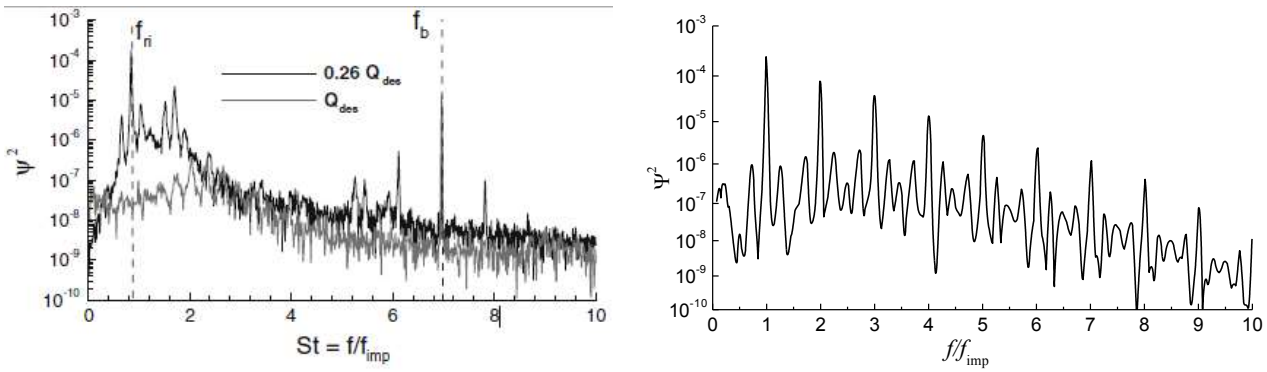

(a) the experimental results at Q/Q_d=0.26 [10] (b) the simulation results at Q/Q_d=0.26

Figure 10 The spectral of pressure fluctuation

5.2 Cell patterns

The shape of the unstable cells are compared to the ones obtained in the experimental results [11], in term of radial velocity distribution for Q/Q_d = 0.26 (Figure 11). For this flow rate it seems that the results of the simulation are in a very good agreement with experiments, concerning the global shape of the unstable cell (it should be noticed that the color level are reversed in the experimental results compared to ths simulation ones because the frame was also reversed (the tangential velocity at the diffuser inlet is assumed to counterclockwise in the simulation. It is clockwise in the PIV map).

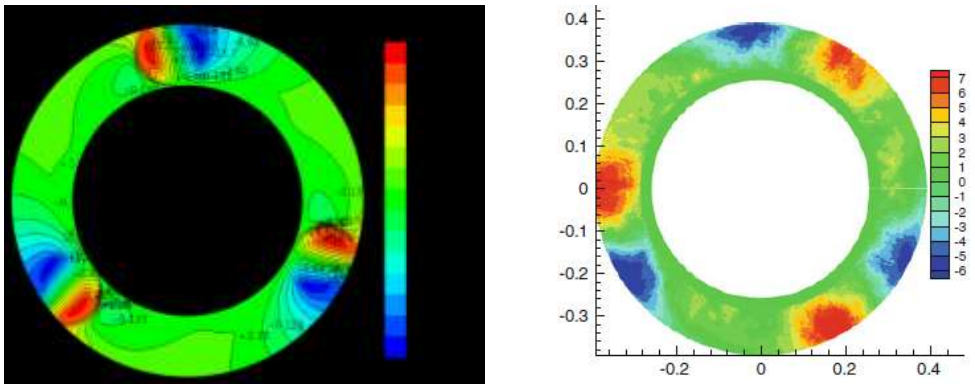

(a) calculation results (b) experimental results [11]

Figure 11 The radial velocity for the flow rate is Q/Q_d=0.26

The numerical and experimental values of radial velocities for the two radii (R=320mm and R=370mm) at the flow rate Q/Q_d=0.26 are given in Figures 12 and 13 depending on the angle position. Three peaks can be observed for the two-dimensional simulations and for the experimental measurements, which are due to the presence of the three cells. It can be observed that these three peaks are of similar amplitude.

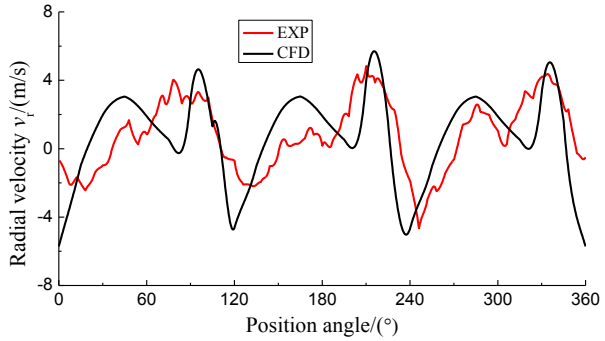

Figure 12 The radial velocity for radius R=320mm

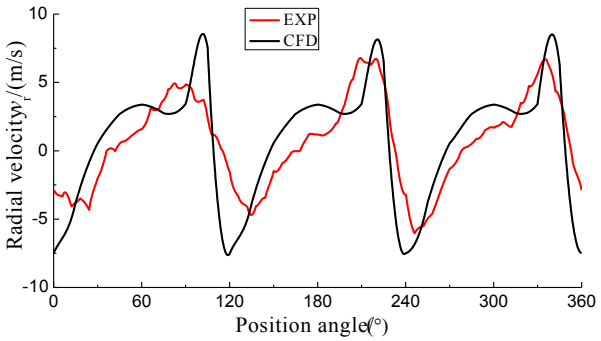

Figure 13 The radial velocity for radius R=370mm

5.3 Critical flow angle

The critical flow rate and the angle of rotating stall occurrence (flow angle at which the instability develops) for the three methods, the numerical simulation, the experiments and the linear stability analysis [16], are given in Table 2. The prediction of their value are very close for numerical and analytical approaches, but they both underestimate the value of the flow angle,and consequently they overestimate the flow rate at which the instability will first develops. These differences could be attributed to :

- The hypothesis (2D flow, axisymmetric boundary condition at inlet) used for the analytical and the numerical approaches
- A bad estimation of the experimental flow angle which is not measured but estimated by the calculation of the velocities' triangle at impeller outlet. An experimental campaign is programmed in the next future to evaluate its value.

	Critical flow rate	Critical flow angle	Number of stall cells
Numerical simulations	Q/Q_d=0.61	$\tilde{\alpha} = 6.1°$	n=4
Experiments	Q/Q_d=0.76	$\tilde{\alpha} = 8.1°$	n=4
Linear stability analysis	Q/Q_d=0.58	$\tilde{\alpha} = 5.7°$	n=4

Table. 2 The occurrence of the rotating stall

5.4 Characteristics of rotating stall

The propagation speed and the number of stall cells are important characteristics of the rotating stall. The propagation speed of the rotating cells $\omega = 2\pi f_{rs}/n$. f_{rs} is the dominated frequency, n the number of stall cells. The calculation results are once again compared with the experimental ones [10-12] and to those of the linear stability analysis [16] as shown in Figures 14 and 15. It has to be noted that, in the experiments, in many cases, several concurrent modes could be observed simultaneously. The values reported in Figure 14 correspond to the dominant mode (the one with the highest amplitude). The linear stability theory could also predict the arising of several modes, depending on the flow rate; this is the most unstable mode which is reported on Figure 14 (the one with the greatest growth, that is the rate at which the mode develops, according to linear stability analysis). On the contrary, one single mode was observed in the numerical simulation. In Figure 14, it can be observed, that when the flow rate is decreased from stable to unstable conditions, the analytical prediction and the numerical simulation predict correctly that the first unstable mode developped is the mode n=4. But when the flow rate decreases, the simplified approach fails to predict correctly the correct number of modes, except for the lowest flow rates predicted. This means that, problably, the 3D effects, as well as the velocity profile at inlet could have an effect on the development of the instability. New simulations with more realistic velocity profiles will be managed in the next future.

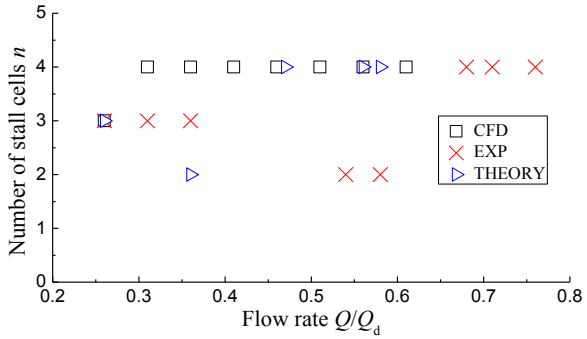

Figure 14 Number of stall cells

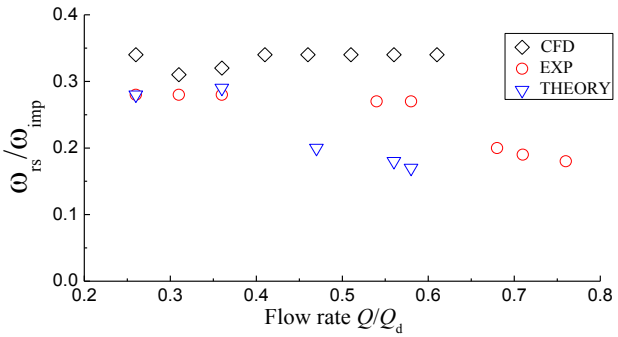

Figure 15 Propagation speed

Figure 15 shows the evolution of the propagation speed of the most dominant mode in the diffuser. First of all, it has to be noted that the order of the propagation speeds predicted by the linear stability analysis and the 2D numercial simulations have the same order of magnitude as what is oberved in the experiments. But, for numerical simulations, the velocity is systematically overestimated and is nearly constant, whereas in the experiments, there is an increase of the velocity with the decrease of the flow rate. On the contrary, this trend is well predicted by the analytical approach, but the velocities are underestimated except fot the lowest flow rates.

It has to be said that, in most experiments, there was not a single mode which was observed, but several competitive ones. On the contrary, the numerical simulations are predicting the arising of only one single mode. The linear stability analysis could predict the arising of several modes, but their evolution is supposed to be independent from the evolution of the others. The interaction of several unstable modes could have an influence on their velocities, in the experiments.

Besides, the effect of the development of boundary layers, which does exist in the real case, are ignored by the two simplifed approaches.

4. CONCLUSIONS

In this paper, the ability of two simplified approaches to try to predict the arising of rotating stall in the vaneless diffuser of a radial flow pump are evaluated and compared to the existing experimental results [10-

11]. The first one is a linear stability analysis which is available in litterature [8, 16]. The second one is based on a 2D numerical simulations of the vaneless diffuser with a simplified boundary condition at inlet where the velocity is supposed to be axisymmetric.

Both simplified approaches are able to predict the arising of rotating instability. The shape and the amplitude of the instability, obtained in a numerical simulation, are very close to the experiments. Concerning the arising of the instability, the critical flow angle (the inlet flow angle under which the instability develops) seems to be overestimated by the two simplified approaches.

Both methods agree to predict that the first mode developped is the mode n=4. But, when the flow rate decreases, they fail to predict the correct dominant modes (except at very low flow rates).

The two simplified approaches are predicting the good order of magnitude for the propagation speed. But the numerical calculations are systematically overestimating the experimental data whereas the analytical method is underestimating them, except for the lowest flow rate tested experimentally.

The main differences between the two simplified approaches compared to the experiments are the following :

- The effect of the boundary layer are neglected,
- The velocity at the inlet is supposed to be axisymmetric,
- The interaction between the modes are not taken in account in the linear stability analysis and not observed in CFD,
- There is a doubt about the value of the experimental value of the flow angle at diffuser inlet.

To try to improve the simplied approaches, several new works are forecasted in the following months :

- An experimental campaign to measure the flow angle and the boundary layer thickness,
- An extension of the linear stability analysis to non linear interaction between modes,
- New CFD Calculations with more realistic inlet boundary conditions.

NOMENCLATURE

σ	Slip factor	
v_θ	Tangential velocity	m/s
v_r	Radial velocity	m/s
Q	Flow rate	m^3/s
R_2	Impeller outlet radius	mm
R_1	Impeller inlet radius	mm
Z	Number of impeller blades	
b_2	Exit blade height of the impeller	mm
β_2	Outlet blade angle	deg
N	Rotation speed	rpm
Q_d	Design flow rate	m^3/s
Re	Reynolds number	
R_3	Inlet Radius of the diffuser	mm
R_4	Oultet Radius of the diffuser	mm
h	Constant height of the diffuser	mm
f	Frequency	Hz
n	Number of rotating stall cells	
S_u	Thickness of impeller blades	mm
D_2	Diameter of impeller tip	mm
u_2	Impeller tip tangential velocity	m/s

ACKNOWLEDGEMENTS

The researchers gratefully acknowledge the financial support extended by the Priority Academic Program Development of Jiangsu Higher Education Institutions and the China Scholarship Council as well as the academic support of Ecole Centrale de Lille and Arts et métiers ParisTech.

REFERENCES AND CITATIONS

[1] Jansen, W. (1964). Rotating stall in a radial vaneless diffuser. J Basic Eng, 86, pp. 750-758.

[2] Senoo, Y. and Kinoshita,Y. (1977). Influence of inlet flow conditions and geometries of centrifugal vaneless diffusers on critical flow angle for reverse flow. ASME Journal of Fluids Engineering, vol. 99, pp. 98–103.

[3] Frigne, P. and Van den Braembussche, R. (1984). Distinction between different types of impeller and diffuser rotating stall in a centrifugal compressor with vaneless diffuser. ASME Journal of Engineering for Gas Turbines and Power, vol. 106, no. 2, pp. 468–474.

[4] Dou, H. S. and Mizuki, S. (1998). Analysis of the flow in vaneless diffusers with large width-to-radius ratios. ASME Journal of Turbomachinery, vol. 120, pp. 193–201.

[5] Abdelhamid, A. N. (1980, March). Analysis of rotating stall in vaneless diffusers of centrifugal compressors. In ASME 1980 International Gas Turbine Conference and Products Show (pp. V01BT02A089-V01BT02A089). American Society of Mechanical Engineers.

[6] Fringe, P. and Van den Braembussche, R. (1985). A theoretical model for rotating stall in the vaneless diffuser of a centrifugal compressor. ASME J Eng Gas Turbine Power, 107(2), pp. 507–513.

[7] Ishida, M., Sakaguchi, D. and Ueki, H. (2001). Suppression of rotating stall by wall roughness control in vaneless diffusers of centrifugal blowers. Journal of Turbomachinery, 123, pp. 64–72.

[8] Tsujimoto, Y., Yoshida, Y. and Mori, Y. (1996). Study of vaneless diffuser rotating stall based on two dimensional inviscid flow analysis. ASME J Fluids Eng, 118, pp. 123–127.

[9] Moore, F. K. (1989). Weak rotating flow disturbances in a centrifugal compressor with a vaneless diffuser. ASME Journal of Turbomachinery, 111, pp. 442–449.

[10] Dazin, A., Coudert, S., Dupont, P., Caignaert, G., Bois, G. (2008). Rotating instability in the vaneless diffuser of a radial flow pump. J Thermal Sci, 17(4), pp. 368–374.

[11] Dazin, A., Cavazzini, G., Pavesi, G., Dupont, P., Coudert, S., Ardizzon, G., Caignaert, G., Bois, G. (2011). High-speed stereoscopic PIV study of rotating instabilities in a radial vaneless diffuser. Exp Fluids, 51, pp. 83–93.

[12] Pavesi, G,. Dazin, A., Cavazzini, G., Caignaert, G., Bois, G., Ardizzon, G. (2011). Experimental and numerical investigation of unforced unsteadiness in a vaneless radial diffuser. In: Proceedings of the 9th european conference on turbomachinery-fluid dynamics and thermodynamics (Turkey), pp. 625–636.

[13] Wuibaut, G., Dupont, P., Bois, G., Caignaert, G., Stanislas, M. (2002). PIV Measurements in the impeller and the vaneless diffuser of a radial flow pump in design and off design operating conditions. ASME Journal of Fluids Engineering, vol 124, pp.791-797.

[14] Ljevar, S. (2007). Rotating stall in wide vaneless diffusers. PhD. Thesis. Eindhoven University of Technology.

[15] Ljevar, S., de Lange, H. C., van Steenhoven, A. A. (2006). Two-dimensional rotating stall analysis in a wide vaneless diffuser. Int J Rotat Mach, Article ID 56420, pp. 1–11.

[16] Heng, Y. G., Dazin, A., Ouarzazi, M. N., & Si, Q. R. (2016, November). Experimental Study and Theoretical Analysis of the Rotating Stall in a Vaneless Diffuser of Radial Flow Pump. In IOP Conference Series: Earth and Environmental Science (Vol. 49, No. 3, p. 032006). IOP Publishing.